Diagram of the aging dynamics in laponite suspensions at low ionic strength

F. Schosseler,[1] S. Kaloun,[2,3] M. Skouri,[3] and J. P. Munch[2]
[1]*Institut Charles Sadron, UPR 22, 6 rue Boussingault, 67083 Strasbourg Cedex, France*
[2]*Institut de Physique et Chimie des Matériaux de Strasbourg, UMR 7504, 23 rue du Loess, Boîte Postale 43, 67034 Strasbourg Cedex, France*
[3]*Laboratoire d'Electronique et d'Instrumentation, Faculté des Sciences Semlalia, Université Cadi ayyad, Marrakech, Morocco*
(Received 3 November 2005; published 9 February 2006)

We measure the dynamic structure factor (DSF) of probe particles embedded in an aging laponite suspension quenched by cessation of shear and the associated relaxation time τ as a function of wave vector q and aging time t_w. The different q dependences measured in the successive exponential and full aging regimes, respectively, $\tau \sim q^{-2}$ and $\tau \sim q^{-1.25}$, yield a weak positive q dependence for the aging time t_{wc} corresponding to the crossover between the two regimes. This implies that the full aging behavior is first seen when investigating large length scales in the aging suspension. We propose a qualitative diagram of the aging dynamics and discuss the features of the DSF of the probes and of the matrix in the two aging regimes. Consistently with the idea that the full aging regime is first observed when probing large length scales, t_{wc} is markedly shorter when the motion of the probes is tracked instead of the collective fluctuations of concentration in the matrix. The exponential aging regime is most probably related to the liquid-glass transition induced by the cessation of shear rather than to the aging of a glass.

DOI: 10.1103/PhysRevE.73.021401 PACS number(s): 82.70.Dd, 64.70.Pf, 61.20.Lc, 83.85.Ei

INTRODUCTION

The physical aging of colloidal systems quenched in an out of equilibrium state has attracted a wide interest in the last decade [1]. Usually quenching a physical system at thermodynamic equilibrium involves the abrupt change in one parameter of the phase diagram, e.g., the temperature, to drive the system in a region where the dynamics is increasingly slowing down. For repulsive colloidal suspensions, however, the main parameter governing the dynamics is the effective volume fraction occupied by the colloids [2,3] and usually its value cannot be easily switched to enter the region with increasingly slow dynamics. For such systems, a common trick is to prepare them under shear, i.e., in stationery nonequilibrium conditions, and to quench them by stopping the flow [4–9]. An aging time t_w can then be defined by the time elapsed since the cessation of shear.

Laponite synthetic clay suspensions are a typical example of colloidal suspensions exhibiting aging behavior at low weight fractions about a few percent. The presence of long range interactions and the strong anisotropy of the particles explains why colloidal glasses and gels can be obtained at such low weight fractions [10–21] in contrast with the behavior observed for suspensions of hard or soft spheres. The laponite particles that constitute the clay are disklike objects about 1 nm thick with a diameter about 30 nm. The interactions between laponite particles depend on both the pH and the ionic strength, and are still a matter of debate [10–21]. In aqueous suspensions at $p\mathrm{H}=10$, their surface is negatively charged while their rim can bear positive charges in more acidic conditions [13]. In addition, van der Waals interactions favor the stacking of the disks while quadrupolar interactions favor T-shaped configurations [11,15]. At low ionic strength, $I=10^{-4}$ mol/L, and $p\mathrm{H}=10$, the net balance of the forces is repulsive and the osmotic pressure of the suspensions is positive [19]. At higher ionic strength $I \geqslant 10^{-3}$ mol/L, the net balance appears to be negative and the platelets tend to aggregate and to form gels [17,21]. Recent Brownian dynamics simulations have confirmed that the detailed structure of the laponite suspensions depends on the repartition of charges on the platelets and on the ionic strength [20]. For weight fractions between about 0.03 and 0.05, depending on the ionic strength, steric effects play an increasing role and a transition to a nematic state has been observed [12,23].

Experimental observations show that, nearly whatever the conditions, the properties of laponite suspensions are evolving with time. At low ionic strength, the suspensions are liquids showing a long time evolution for weight fractions ϕ above about 0.003 [22]. The aging dynamics of laponite suspensions in pure water quenched by cessation of shear flow have been studied in some details.

Studies by rheological techniques have in particular shown that the elastic moduli increase with aging time and that the system transforms gradually from a flowing liquid to a soft solid that can sustain its own weight without flowing [4,24–27]. This increase in the elastic moduli occurs without expulsion of the solvent, which would be a signature for a gelation through an aggregation mechanism.

The aging dynamics can also be followed by measuring the time evolution of the dynamic structure factor (DSF) of the laponite suspension [22,24,26,28–31]. Dynamic light scattering experiments with standard correlation techniques have shown two relaxation mechanisms.

A fast relaxation with time scale τ_1 in the range of 10 μs at a scattering wave vector $q \approx 20\ \mu\mathrm{m}^{-1}$ corresponds to the decorrelation by the collective diffusive motion of the particles and scales as $\tau_1 \sim q^{-2}$ [24,26,29] except in Ref. [28] where it was reported as independent of the scattering wave vector and attributed to the rotational diffusion of the clay particles. This time was found to be independent of aging time until a recent paper [22] reported the existence of two

aging behaviors according to the concentration: τ_1 was found constant above a weight fraction $\phi^* \approx 0.015$ and somewhat increasing with aging time for smaller concentrations.

The second relaxation is very sensitive to the aging time [22,24,26,28,29]. It has been usually described as a stretched exponential decay [25,30] with an exponent β varying between about 0.7 for short t_w and about 0.2 for larger t_w. Its relaxation time τ_2 has been reported to scale like q^{-2} [22,26], and to grow exponentially with t_w [26] or like $\exp\{B[t_w/(t_w^\infty - t_w)]\}$ [22], where B and t_w^∞ are two fitting parameters that allow us to obtain master curves for the evolution of τ_2 and β with t_w. These master curves are different below and above ϕ^* [22]. However as the aging still proceeds, the structure factor does no longer decay to zero and exhibits a pseudoplateau. This indicates that the experiments do not probe large enough time scales to measure the longest relaxation time of the system. The analysis of the DSF becomes then difficult since nonergodic effects play a role. Only ensemble-average measurements then make sense if no simplifying assumptions about the structure and the dynamics are used. Typically τ_2 values below 0.1 s can be measured by standard techniques before the pseudoplateau appears and this corresponds to aging times t_w about several hours ($10^4 - 10^5$ s) above ϕ^* and about a few months (10^7 s) below ϕ^* for q values about 20 μm^{-1} [22,26,28].

To measure all the relaxation processes in the system with an ensemble average would require prohibitively long measurement times with standard correlators. New techniques involving multispeckle correlation spectroscopy [30–35] provide the means to study the aging system for relaxation times τ_2 as long as 10^3 s. For pure laponite systems, this has been done using light [30], $8 < q(\mu m^{-1}) < 25$, or x ray [31], $50 < q(\mu m^{-1}) < 300$, sources. In these conditions, where the ensemble-averaged DSF is measured on time scales long enough to allow its decay to zero, two different aging regimes were successively observed in the light scattering experiments [30]: first an exponential aging regime, where the relaxation time grows exponentially with t_w, followed by a full-aging regime, where $\tau_2 \sim t_w^{1.0\pm0.1}$. In the latter regime, the DSF is found to be a compressed exponential with $\beta \approx 1.35 \pm 0.15$ and the relaxation time varies unusually with the scattering wave vector as $\tau_2 \sim q^{-1.3\pm0.1}$. This compressed exponential shape of the DSF has been confirmed at smaller length scales by x ray scattering experiments [31] with an exponent $\beta \approx 1.5$, a faster than linear growth, $\tau_2 \sim t_w^{1.8\pm0.2}$, and a weaker q dependence for the longest relaxation time, $\tau_2 \sim q^{-0.9\pm0.1}$. Typical orders of magnitude are $10 - 10^4$ s for τ_2 when t_w is about $10^3 - 10^5$ s for weight fractions in the range $\phi \approx 0.03 - 0.035$, depending on q [30,31].

A drawback of multispeckle correlation spectroscopy via charge-coupled device (CCD) detectors is the finite short time resolution that is limited by the frame rate of the CCD cameras. Thus the short aging time behavior is missing with these techniques. One way to overcome this limitation is to track some effective viscosity of the medium by following the motion of tracer particles [36,37] that are large enough to shift the smallest time scale, associated with their Brownian motion in a low viscosity liquid, in the window of the smallest relaxation times measurable with usual cameras, i.e., about 1 s.

This approach was first used in laponite suspensions with concentrations of the tracers large enough to enter the multiple scattering regime of diffusive wave spectroscopy (DWS) [29,38–40]. With this technique, the motion of the tracers on distances smaller than about 10 nm is probed and the dependence on the scattering wave vector is lost. The decrease of the ensemble-averaged DSF measured by the CCD techniques could be described by a compressed exponential with $\beta \approx 1.5$, and τ was found to increase quasilinearly with the aging time, $\tau \sim t_w^{1.05\pm0.02}$ [29]. This behavior closely resembles that of the full-aging regime for the pure laponite system. We emphasize that τ is the relaxation time associated with the decorrelation brought by the motion of the tracers embedded in the laponite matrix, and is distinct from the time τ_2 characterizing the long time relaxation of the laponite suspension discussed above. In the multispeckle DWS experiments, typical orders of magnitude for τ are $10 - 10^3$ s for t_w in the range $10^3 - 10^5$ s [29]. On the other hand, similar DWS experiments with standard correlation techniques [41] measured τ values in the range $10^{-3} - 10^{-1}$ s for aging times t_w below a few 10^3 s. In this range of aging times, it was found that $\tau \approx \tau_2(q \approx 20\ \mu m^{-1})$ and that both times grow exponentially with t_w, in parallel with the complex viscosity η^*. However, for larger aging times, the growths of τ_2 and η^* appear to not follow the same law [26].

More recently, we measured the ensemble-averaged DSF of dilute tracer particles in aging laponite suspensions [42]. We observed two successive regimes as a function of the aging time. In the first one the DSF of the tracers is a single exponential with a characteristic time τ growing exponentially with t_w and scaling like q^{-2}. Beyond a crossover aging time t_{wc} the DSF can be described by a compressed exponential with $\beta \approx 1.5$ while τ grows linearly with t_w and scales like $q^{-1.25\pm0.1}$. This behavior was measured on large length scales, $0.8 < q(\mu m^{-1}) < 3$, and typical τ values are in the range $1 - 10^4$ s for t_w values between 10^2 and 10^4 s. Thus the behavior of $\tau(t_w)$ mimics that of $\tau_2(t_w)$ and this indicates that the aging behavior of the matrix can be probed by the tracers. However, there remain interesting questions concerning the length scales probed in the two types of experiments and in particular we want to discuss here the crossover between the two aging regimes as a function of the scattering wave vector.

EXPERIMENTAL

Sample preparation. The samples were prepared as previously described [29,30,42]. The oven-dried laponite RD (Southern Clay Products, Gonzales, TX) was dissolved under stirring in deionized water for 2 h, resulting in solutions with $p\mathrm{H} \approx 9.8$ and ionic strength $I \approx 10^{-4}$ mol/L [29]. The clarified solutions were then filtered through 0.45 μm cellulose acetate filters (Millipore), in order to breakup particle aggregates that would otherwise lead to spurious small angle scattering [25]. The polystyrene tracer particles (Polysciences, nominal radius $R = 0.5\ \mu$m) were added after the filtration under stirring. The age t_w of the samples is measured from the time where the stirring is stopped and the scattering cell (1 mm optical path) filled through a syringe.

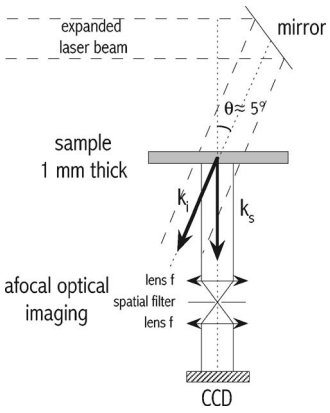

FIG. 1. Sketch of the multispeckle experimental setup at fixed scattering wave vector: $\mathbf{k_i}$ and $\mathbf{k_s}$ are the incident and the scattered wave vectors, respectively.

The volume fraction of the latices is kept to 10^{-4}. In these conditions, their scattering contribution remains much larger than that of the host matrix (intensity ratio $\approx$3230) and we can measure the DSF of isolated particles in the single scattering regime.

Some features affect the reproducibility of sample preparation. The filtration can change slightly the concentration depending on the amount of ill-dispersed clay aggregates but the most critical feature is the difficulty to reproduce strictly the flow conditions along the preparation: stirring, flow through the filter, stirring, filling of the cell with the syringe. Similarly, comparison with different sets of experiments published earlier by us or different groups can be difficult. In particular, for experiments performed without added probes, t_w is usually defined from the time where the sample is filtered into the scattering cell. Thus, although the time origin in itself bears only a negligible error compared to the aging times that are investigated, the starting state of the system is probably difficult to reproduce exactly, owing to its dependence to the flow conditions. As a consequence, we observed random fluctuations by a factor typically about 2 in the aging kinetics of the samples. Although these fluctuations do not change the general features of the aging behavior, they tend to blur the effects of concentration on the aging kinetics, which are now well established [22,28], and they make necessary the use of a setup that can measure simultaneously a range of scattering wave vectors if the influence of the latter parameter is under scrutiny.

Dynamic light scattering. We have used two different setups. In the first one (Fig. 1), a fraction of the volume illuminated by the expanded collimated incident beam (wavelength 4880 Å), is imaged by an afocal optical system with a magnification about unity onto the CCD detector of a camera that is positioned at a given angle off the axis of the incident beam ($\theta \approx 5°$ measured from the Brownian diffusion of the tracer particles in water). The intensity autocorrelation function is built in real time as described in Ref. [35] from image frames exposed for 40 ms. In this setup, each pixel on the CCD (752×582, 8.6 μm $\times$ 8.3 μm) sees a different scattering volume under the same transfer wave vector $\mathbf{q}$ ($|\mathbf{q}| \approx 1.5\ \mu\text{m}^{-1}$), which allows one to measure with very good statistics the ensemble-averaged DSF as a function of the aging time since, by an appropriate choice of the optics, one pixel area corresponds roughly to one coherence area. This setup is best suited for the accurate characterization of the shape of the DSF.

In the second setup, which has been detailed elsewhere [43], the same scattering volume is seen by each pixel under a unique transfer wave vector $\mathbf{q}$ differing in module and/or orientation. It is essentially the same geometry as in small angle neutron or x ray scattering with the detector centered on the incident beam and protected by a beam stop. The intensity correlation functions are ensemble-averaged on annular regions centered on the position of the incident beam. The characteristics of the dynamic light scattering experiment on this setup have been explained in the previous paper. The scattering wave vectors are comprised between 0.79 μm^{-1} and 3.14 μm^{-1}, with a typical angular resolution $\Delta q/q \approx 0.2$. The characteristic area of the speckles is about 25 pixels. It follows that the averages for the ensemble-averaged time correlation functions are obtained on a number of coherence areas comprised between about 220 and 1400. Therefore the statistics on the ensemble-averaged DSF are poorer than in the first setup. Only a characteristic decay time τ can be obtained with this setup. On the other hand, the study as a function of the scattering wave vector can be done in a single experiment, which eliminates the problem of fluctuations in the aging kinetics between different samples.

The calibration of both setups was checked by measuring the dynamic structure factor of the lattices in water and in viscous wormlike micellar solutions. The results obtained with these ergodic stationary systems were found in satisfactory agreement with those obtained with a standard dynamic light scattering setup using a goniometer, a photomultiplier, and a hardware correlator.

Data analysis. Throughout the present paper, the correlation time τ has been simply defined as the time at which the DSF has decayed by a factor $1/e$ as in the previous paper [42]. The use of the present operative definition allows one to decouple the mean decay time τ from the value of the exponent β in the case where the DSF is a compressed exponential and to obtain comparable τ values for both setups.

RESULTS

Figure 2 shows the variation of the correlation time with the aging time for different clay concentrations at a fixed scattering wave vector $q = 1.5\ \mu\text{m}^{-1}$. For $0.025 < \phi < 0.03$, the same features as reported previously for $\phi = 0.0275$ [42] are observed: as t_w increases, an initial exponential growth of the decay time, $\tau = \tau_0 \exp(\gamma t_w)$, is followed by a linear increase of τ, $\tau = \alpha t^{v}$ with $v \approx 1.04 \pm 0.06$. These two behaviors correspond respectively to the so-called exponential and full-aging regimes [30]. These two regimes are also distinguished by the shape of the dynamic structure factor $f_p(q,t)$ [42]: in the exponential aging regime, it is a simple exponential associated with a diffusive behavior, $f_p(q,t) = \exp[-t/\tau(q)]$, while in the full-aging regime, it is best described by a compressed exponential, $f_p(q,t) = \exp\{-[t/\tau(q)]^{\beta}\}$ with $\beta = 1.5 \pm 0.1$ [42], which corresponds to a super-diffusive regime.

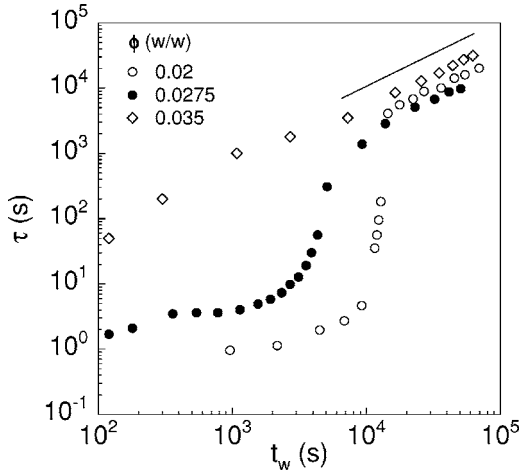

FIG. 2. Variation of the decay time τ with the aging time t_w for different laponite weight fractions ($q=1.5\ \mu m^{-1}$). The straight line corresponds to a power law with exponent equal to unity.

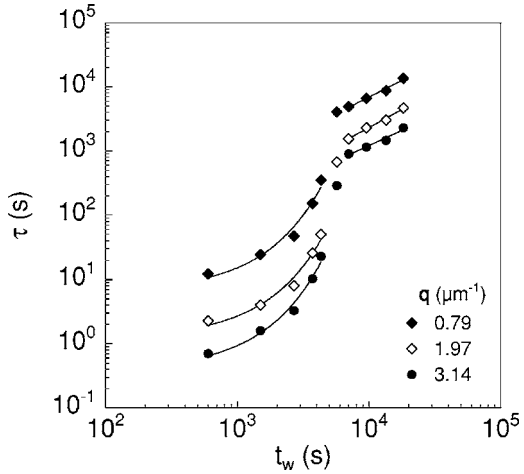

FIG. 4. Variation of the decay time τ with the aging time t_w for different scattering wave vectors ($\phi=0.0275$). The curved and straight lines are respectively exponential and power law fits.

The aging time t_{wc} corresponding to the crossover between the two regimes tends to decrease as the concentration increases although this trend can be masked by the fluctuations between samples. Here we crudely estimated t_{wc} as the typical aging time where the increase of τ can no longer be described by a single exponential but is not yet linear with t_w. A more precise definition would demand a model for the variation of τ as a function of t_w in the crossover region. As shown in Fig. 3, the experimental values of t_{wc} plotted as a function of ϕ are consistent with the exponential decay proposed earlier for the aging time T_g beyond which a frozen intensity is measured [28] or for the time t_w^∞ in the empirical fit of $\tau_2(t_w)$ proposed by Ruzicka *et al.* [22] for the exponential regime. If we adopt the same functional dependence then we find $t_{wc} \approx 5.5\times 10^{-7}\exp(-254\phi)$. Eventually, for $\phi=0.035$, only the full aging regime is observed. It can be noticed that, for this concentration, the results should be considered with some caution since τ is of the same order of magnitude as t_w. Since the typical duration of a measurement of $f(q,t)$ has the same magnitude as τ, this means that the quasistationery approximation is not satisfied. Therefore the data for this concentration will not be discussed in detail.

The same succession of the exponential and the full-aging regimes is observed whatever the scattering wave vector (Fig. 4). It is already clear from these data that the crossover time t_{wc} depends slightly on q, since for $t_w=5700$ s, the τ value belongs already to the full-aging regime for $q=0.79\mu^{-1}$, while it is in between the two regimes for the two other wave vector values. As shown in Fig. 5, the decay time exhibits a different power law dependence on the wave vector in the exponential regime, $\tau \sim q^{-2.02\pm0.05}$, and in the full-aging regime, $\tau \sim q^{-1.25\pm0.1}$ [42].

In the exponential aging regime, this q dependence is entirely contained in the coefficient τ_0: the coefficient γ characterizing the exponential growth of τ with t_w is independent of q (Fig. 6). This is consistent with the idea that immediately after the quench of the system at $t_w=0$ the tracers should probe a viscosity η that is close to its value before the

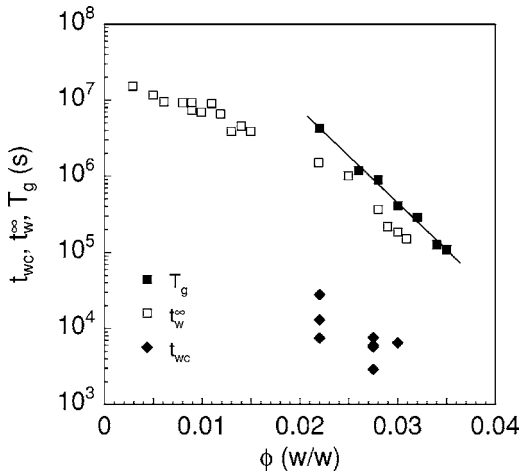

FIG. 3. Concentration dependence of t_{wc}, T_g, associated with the onset of frozen intensity [28], and t_w^∞, associated with the apparent divergence of τ_2 in the exponential aging regime [22]. The straight line is the exponential fit proposed by Kroon *et al.* [28].

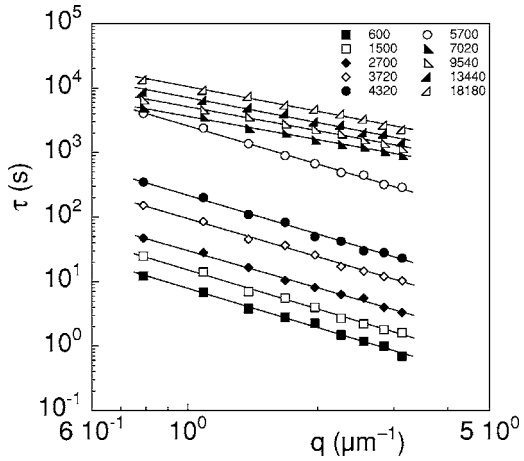

FIG. 5. Scattering wave vector dependence of the decay time τ for different aging times ($\phi=0.0275$). The straight lines show the corresponding power law fits.

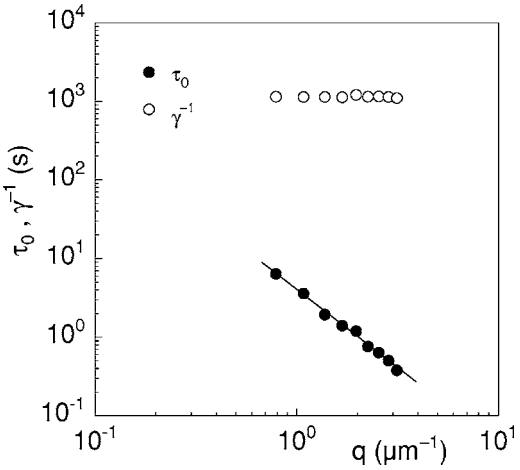

FIG. 6. Scattering wave vector dependence of the fitting parameters describing the evolution of the decay time τ in the exponential aging regime, $\tau=\tau_0 \exp(\gamma t_w)$. The straight line is a power law fit with exponent −2.01 ($\phi=0.0275$).

quench. Indeed, the diffusion coefficient D deduced from $D=(q^2\tau_0)^{-1}$ yields from the Stokes-Einstein relationship, $D=kT/(6\pi\eta R)$, viscosity values about a few mPa s, which are well consistent with the values expected for an aqueous laponite dispersion at these volume fractions. Here k is the Boltzmann constant and T the room temperature.

In the full-aging regime, the exponent υ is 1.04 ± 0.06 when ϕ is varied at fixed q (Fig. 2) and is 1.05 ± 0.06 when q is varied at fixed ϕ, as in Fig. 4. These values are averages from the values obtained for, respectively, all the concentrations and all the scattering wave vectors probed in the experiments. Therefore, it can be concluded that υ does not depend on the concentration and on the scattering wave vector, within the experimental accuracy. Then the dependence of τ on these parameters is contained in the coefficient $\alpha(q,\phi)$.

Due to the very limited experimental ϕ range available and to the fluctuations between samples, it was not possible to deduce a functional dependence for $\tau_0(\phi)$, $\gamma(\phi)$, and $\alpha(q,\phi)$.

DISCUSSION

Crossover aging time

We can summarize the experimental behavior of τ in the two aging regimes as

$$\begin{aligned}\tau(\phi,t_w,q,R) &= [D(\phi,R)q^2]^{-1}\exp[\gamma(\phi)t_w], \quad t_w < t_{wc} \\ &= [\ell(\phi)q]^{1.25}h(\phi,R)t_w, \quad t_w > t_{wc} \end{aligned} \tag{1}$$

These expressions show explicitly the functional dependence on the parameters (ϕ,t_w) of the system and on the parameters (q,R) of the experiment that probes the physical aging of the system. We note that the latter parameters define two length scales on which this aging is measured.

For the full-aging regime, we have set $\upsilon=1$ within the experimental accuracy to simplify the further discussion. We have also explicitly introduced a characteristic length of the system, $\ell(\phi)$, which depends *a priori* on the concentration, to make the function $h(\phi,R)$ dimensionless. We note that $h(\phi,R)$ should be simply proportional to R for continuity at t_{wc}. Splitting the dependence on the concentration in two functions is further justified by the fact that q^{-1} and R can *a priori* be two different length scales, although they are the same order of magnitude in our experiments, $qR\approx1$. Their ratio has been varied by probing the small excursion of large probe particles in the DWS experiments [24,26]. Although it would be interesting to also vary this ratio by changing the size of the probes, in the present state of the experimental setups it is however difficult to achieve: larger R values would yield sedimentation and smaller ones would prevent the detection of the early stage of the aging process due to the limited frame rate of our CCD cameras.

From Eq. (1), the aging time t_{wc} at the crossover is expected to satisfy

$$7q^{-2}\exp(10^{-3}t_{wc}) = 0.17q^{-1.25}t_{wc} \tag{2}$$

where we have dropped the unknown concentration dependences and the numerical factors follow from typical experimental values when units are μm for q^{-1} and R, and seconds for t_{wc}, ϕ being the weight fraction. This yields

$$e^x = Ax, \tag{3}$$

or equivalently:

$$-xe^{-x} = -1/A \tag{3'}$$

where $x=10^{-3}t_{wc}$ and $A=24q^{0.75}$. Equation (3) can be solved numerically or graphically. Depending on whether A is smaller or larger than e, there are zero or two real solutions, respectively. The smallest solution can be discarded since, remembering that the fastest process should dominate the relaxation, it would correspond to a crossover from a full-aging regime to an exponential aging regime. Alternately, from Eq. (3′), we obtain

$$t_{wc} = -\frac{W(-0.042q^{-0.75})}{10^{-3}}, \tag{4}$$

where $W(z)$ is the Lambert W function yielding the solution for w in $z=we^w$ [44]. In the experimental range available, it follows that the dependence of t_{wc} on ϕ and q can be approximated numerically as

$$t_{wc} \approx 10^7 \exp(-283\phi)q^{0.17}, \tag{5}$$

where the exponential dependence is the empirical law proposed by Kroon *et al.* [28] for the dependence of T_g on ϕ. Apart from a numerical coefficient, this law describes as well the variation of t_w^∞ with ϕ above ϕ^* (Fig. 3). Our data appear at least consistent with this exponential variation and we use it to restore in Eq. (5) an approximate ϕ dependence that cannot be deduced from our results. The experimental weak variations of t_{wc} with the scattering wave vector are consistent with Eq. (5).

The most important information obtained from the experimental results and from the above analysis is that the crossover between the exponential aging regime and the full-aging regime is first observed at small q values, i.e., at large

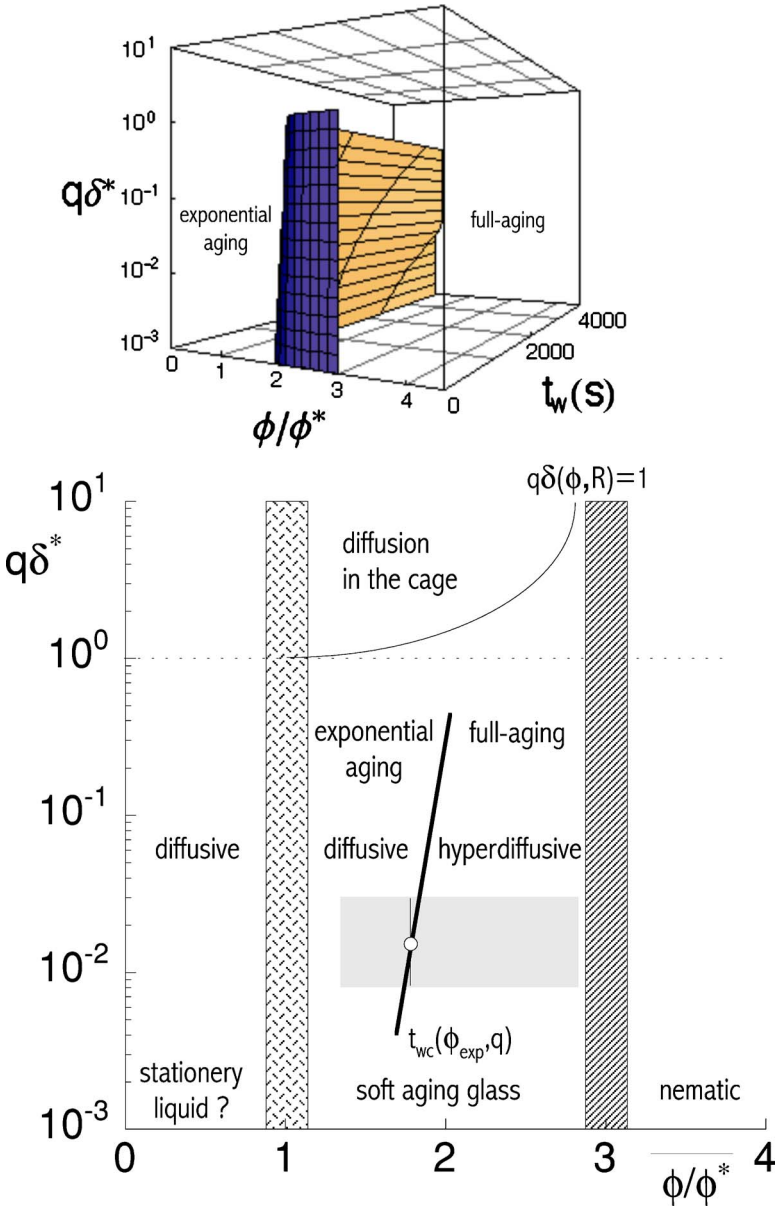

FIG. 7. (Color online) Diagram of aging dynamics for low ionic strength of laponite suspensions as probed by tracers: qualitative shape of $t_{wc}(\phi,q)$ in the $(\phi/\phi^*, t_w, q\delta^*)$ volume (top) and crossover behavior in the $\phi/\phi^* - q\delta^*$ plane (bottom). See text for the details.

length scales. Thus the full-aging regime is first observed when probing large length scales. This stems from the relative exponent magnitude for the q dependence of the relaxation time τ in the two regimes. A hint for this behavior can be seen in the data of Fig. 4 where the transition to the full-aging regime occurs sooner for smaller q values.

The second important point is that the dependence of t_{wc} on q is weak. This makes it very difficult within the available q range and the experimental $\Delta q/q$ resolution to observe the crossover in the power law behavior of $\tau(q)$ at a given aging time t_w (Fig. 5). The experimental exponent seems to jump abruptly from 2 to 1.25. However, conceptually the decrease in the slope should occur first at small q values and then proceed to smaller length scales.

Diagram of the aging dynamics

We are now able to provide a description of the aging dynamics as a function of the three variables ϕ, t_w, and q. It is more convenient to introduce reduced variables. We define ϕ^* as the typical weight fraction above which caging effects are observed and denote δ^* the size of the cage at this concentration. Thus $\phi^* \approx 0.015-0.018$, depending on the ionic strength [10,22]. We note that aging effects can still be present below this weight fraction but with a different mechanism [22]. If the elastic modulus G scales like $G \sim kT/a^3$ at ϕ^*, where $a \approx 30$ nm is here about the typical dimension of the particles in the glass, then $\delta^* \approx (a^3/R)^{1/2}$ [45–47] and it is about 10 nm in our system. The typical dimension of the cage $\delta(\phi,R)$ then decreases as the effective volume fraction increases.

Figure 7 gives a sketch of the diagram of aging dynamics of laponite suspensions at low ionic strength in the $3d$ space of variables (top) and in the $q\delta^* - \phi/\phi^*$ plane (bottom). We note that this diagram depends implicitly on the radius R of the probes through δ^*. The $3d$ graphics shows qualitatively the shape of the surface $t_{wc}(\phi,q)$ delimitating the exponential and the full-aging regimes [Eq. (5)]. A typical experiment

follows a trajectory at constant ϕ/ϕ^* parallel to the t_w axis, starting in the $q\delta^* - \phi/\phi^*$ plane from a point (first setup, fixed q) or from a vertical line (second setup, $q_{\min} < q < q_{\max}$ window). The gray rectangle in this plane (bottom) delimits our experimental range in this paper. The vertical shaded bars show the limits between the regions corresponding to the stationery liquid, the soft aging glass and the nematic phase. The question mark regarding the stationery liquid takes into account the very recent results by Ruzicka *et al.* [22] and an earlier observation by Kroon *et al.* [28]. The thick oblique line is the projection on the $q\delta^* - \phi/\phi^*$ plane of $t_{wc}(\phi_{\exp}, q)$ with $\phi_{\exp}$ corresponding to the experimental value under investigation. For $t_w = t_{wc}(\phi_{\exp}, q_c)$, where $q_{\min} < q_c < q_{\max}$, the exponential (resp. full) aging regime is seen for $q > q_c$ (resp. $q < q_c$). The open circle has coordinates $(\phi_{\exp}/\phi^*, q_c\delta^*)$. In the bottom figure, we have also shown qualitatively the border line $q\delta(\phi, R) = 1$. For larger q values beyond this limit, the diffusion of the tracers inside their cage is probed and no aging should be observed. As the radius R of the probes decreases, the size of the cage increases and the experimental q range (gray area) lies closer to the line $q\delta(\phi, R) = 1$ in the diagram.

Comparison between experiments with or without probes

Figure 8 summarizes the transformation with aging time of the DSF of the probes $f_p(q,t,t_w)$ (top) [42] and gives for comparison the parallel evolution of the DSF of the matrix $f_m(q,t,t_w)$ (bottom) [22,24,26,28–31]. Values are typical for $\phi = 0.03$, $q = 1.5\ \mu\text{m}^{-1}$ (top) and $q = 20\ \mu\text{m}^{-1}$ (bottom). The gray rectangular area represents the experimental time gap not available with the current techniques and has not been investigated up to now. Relaxation times smaller than this window have been measured by standard correlation techniques with no ensemble average (except for Ref. 29). Only multispeckle correlation spectroscopy can probe relaxation times larger than about 1 s in nonstationery systems.

From the evolution of $f_m(q,t,t_w)$, it is clear that the divergence of τ_2 is only an apparent behavior since soon the system enters the full-aging regime where τ_2 has a linear growth. Similarly the probes experience no divergence of τ across the transition between the exponential aging regime and the full-aging regime. As emphasized in Ref. [22], the parameter t_w^∞ is only phenomenological and provides a convenient way to fit with an additional parameter the growth of τ_2 or τ for t_w values closer to t_{wc}. In fact it is often not possible to include data points close to t_{wc} in an exponential fit, which remains a good description of the data at short aging times.

For the purpose of comparison, we can reasonably approximate $\gamma \approx B/t_w^\infty$ and $t_{wc} \approx t_w^\infty$. For $\phi = 0.03$ the evolution of $f_m(q,t,t_w)$ with t_w was described by $t_w^\infty \approx 50\ \text{h} \approx 1.8 \times 10^5$ s and $B \approx 6$ [22], i.e., $B/t_w^\infty \approx 3 \times 10^{-5}\ \text{s}^{-1}$, which should be compared to $t_{wc} \approx 5 \times 10^3$ s and $\gamma \approx 3 \times 10^{-4}\ \text{s}^{-1}$ for the present work where $f_p(q,t,t_w)$ is measured. Thus our systems appear to display a faster evolution in the so-called exponential regime.

One possible explanation for this feature is that the measurement of $f_p(q,t,t_w)$ involves much larger length scales

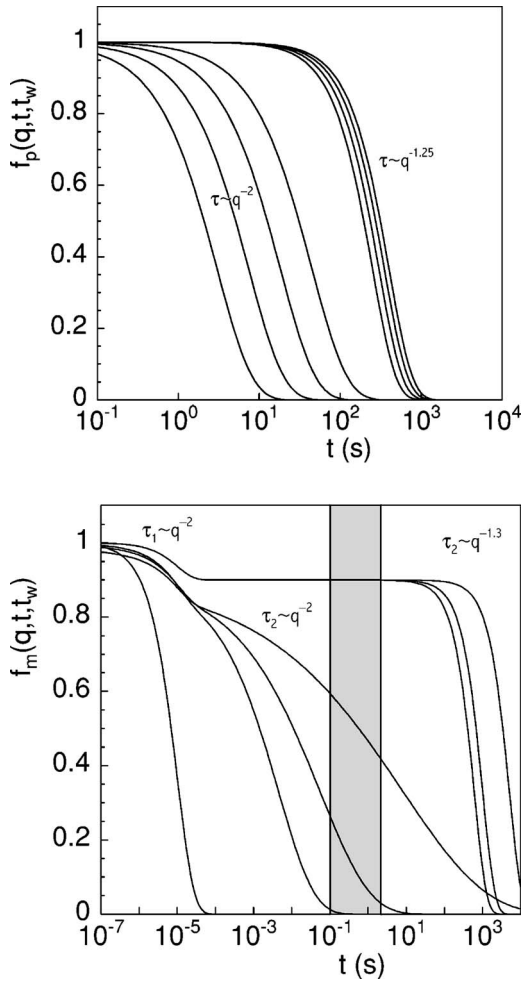

FIG. 8. Schematic evolution with aging time of the DSF for the probes $f_p(q,t,t_w)$ (top, $q = 1.5\ \mu\text{m}^{-1}$) and for the matrix $f_m(q,t,t_w)$ (bottom, $q = 20\ \mu\text{m}^{-1}$). For the probes, $f_p(q,t,t_w) = \exp(-t/\tau)$, $\tau = \tau_0 \exp(\gamma t_w)$ $(t_w < t_{wc})$ or $\exp[-(t/\tau)^{1.5}]$, $\tau = \alpha t_w$, $(t_w > t_{wc})$: $t_w/t_{wc} = 0;\ 0.25;\ 0.5;\ 0.75;\ 1.25;\ 1.5;\ 1.75;\ 2$. For the matrix, $f_m(q,t,t_w) = 0.1 \exp(-t/\tau_1) + 0.9 \exp[-(t/\tau_2)^\beta]$, $\tau_2 = \tau'_0 \exp[Bt_w/(t_w^\infty - t_w)]$, $\beta = 0.6 - (2t_w/3t_w^\infty)$, $(t_w < t_w^\infty)$ [22] or $0.1 \exp(-t/\tau_1) + 0.9 \exp[-(t/\tau_2)^{1.35}]$, $\tau_2 = \alpha' t_w$, $(t_w > t_w^\infty)$ [29,30]: $t_w/t_w^\infty = 0;\ 0.2;\ 0.4;\ 0.6;\ 1.2;\ 2;\ 10$. The numerical coefficients are typical for $\phi = 0.03$. Gray area: experimental time gap forbidden by current techniques.

$(q \approx 1\ \mu\text{m}^{-1}, R = 0.25\ \mu\text{m})$ than those involved in the measurement of $f_m(q,t,t_w)$, since the latter reflect the fluctuations of clay particles concentration as measured with standard light scattering techniques $(q \approx 20\ \mu\text{m}^{-1}, R \approx 0.03\ \mu\text{m})$. This explanation is consistent with the q dependence of t_{wc} discussed above.

One might alternately think that these differences simply reflect the variability in the protocols followed by the different groups for the preparation of the samples. However, measurements of $f_m(q,t,t_w)$ in our group [30] yielded $t_{wc} \approx 10^4$ s for $\phi = 0.035$. For the same concentration, no exponential aging can be observed when $f_p(q,t,t_w)$ is tracked (Fig. 2). Therefore the difference cannot be solely linked to a difference in the preparation of samples.

It remains that, as mentioned in the experimental part, the fluctuations in the initial aging kinetics observed for nominally identical samples (Fig. 3) support the idea that the initial time evolution of the sample is sensitive to the details of the preparation. It follows that the absolute values of τ_0, γ, and α are also sensitive to these details. On the other hand, the q dependences of these quantities are independent of the preparation as well as the value $\upsilon \approx 1$ for the exponent describing the aging for $t_w > t_{wc}$. Large fluctuations are also apparent for B and t_w^{∞} [22], when the DSF of the matrix is measured.

Recently, it was proposed [48] that the exponential regime could correspond to an equilibration of the physico-chemical parameters of the suspension, associated with an increase in the effective volume fraction occupied by the clay particles. The suspension would then enter the full aging regime once some critical value for this effective volume fraction is reached. In fact the dc conductivity is still evolving for large aging times [31] and this means that the interactions between platelets are not stabilized as early as assumed in most studies. Less specifically, it was also proposed [42] that the exponential regime could be related to an effective duration of the quench. The identification of two different exponential aging routes according to the laponite weight fraction [22] gives further support to the idea that the exponential aging regime is more closely linked to the liquid-glass transition than to the glass aging.

CONCLUSIONS

We have measured the DSF of probe particles embedded in the aging matrix and its relaxation time τ. The different q dependences, $\tau \sim q^{-2}$ and $\tau \sim q^{-1.25}$, measured in the two aging regimes, yield a weak positive q dependence for the crossover aging time t_{wc}. This implies that the full aging behavior is first seen when investigating large length scales in the aging suspension. We have proposed a qualitative diagram of the aging dynamics of these suspensions in the (ϕ, q, t_w) space and discussed the features of the DSF of the probes $f_p(q,t,t_w)$ and of the matrix $f_m(q,t,t_w)$ in the two aging regimes. The crossover aging time t_{wc} is markedly shorter when $f_p(q,t,t_w)$ is tracked instead of $f_m(q,t,t_w)$. This is consistent with the idea that the full aging regime is first observed when probing large length scales. In agreement with converging evidence from recent reports [22,42,48], it appears that the exponential aging regime is most probably related to the liquid-glass transition induced by the cessation of shear rather than to the aging of a glass. This means that the glassy state is first observed at large length scales in these mechanically quenched systems, in agreement with the general trend in thermally quenched glasses.

[1] *Soft and Fragile Matter: Nonequilibrium Dynamics, Metastability and Flow*, edited by M. E. Cates and M. R. Evans (IOP, Bristol, 2000).

[2] P. N. Pusey and W. van Megen, Phys. Rev. Lett. **59**, 2083 (1987).

[3] E. Bartsch, M. Antonietti, W. Schupp, and H. Sillescu, J. Chem. Phys. **97**, 3950 (1992).

[4] N. Willenbacher, J. Colloid Interface Sci. **182**, 501 (1996).

[5] T. G. Mason, J. Bibette, and D. A. Weitz, J. Colloid Interface Sci. **179**, 439 (1996).

[6] P. Sollich, Phys. Rev. E **58**, 738 (1998).

[7] P. Sollich, F. Lequeux, P. Hébraud, and M. E. Cates, Phys. Rev. Lett. **78**, 2020 (1997).

[8] S. Fielding, P. Sollich, and M. E. Cates, J. Rheol. **44**, 323 (2000).

[9] M. Cloitre, R. Borrega, and L. Leibler, Phys. Rev. Lett. **85**, 4819 (2000).

[10] A. Mourchid, A. Delville, T. Lambard, E. Lécolier, and P. Levitz, Langmuir **11**, 1942 (1995).

[11] M. Dijkstra, J. P. Hansen, and P. A. Madden, Phys. Rev. Lett. **75**, 2236 (1995).

[12] A. Mourchid, E. Lécolier, H. Van Damme, and P. Lévitz, Langmuir **14**, 4718 (1998).

[13] A. Mourchid and P. Lévitz, Phys. Rev. E **57**, R4887 (1998).

[14] M. Kroon, W. L. Vos, and G. H. Wegdam, Phys. Rev. E **57**, 1962 (1998).

[15] S. Kutter, J. P. Hansen, M. Sprik, and E. Boek, J. Chem. Phys. **112**, 311 (2000).

[16] P. Levitz, E. Lécolier, A. Mourchid, A. Delville, and S. Lyonnard, Europhys. Lett. **49**, 672 (2000).

[17] T. Nicolai and S. Cocard, J. Colloid Interface Sci. **244**, 51 (2001).

[18] E. Trizac, L. Bocquet, R. Agra, J.-J. Weis, and M. Aubouy, J. Phys.: Condens. Matter **14**, 9339 (2002).

[19] S. Bhatia, J. Barker, and A. Mourchid, Langmuir **19**, 532 (2003).

[20] G. Odriozola, M. Romero-Bastida, and F. deJ. Guevara-Rodríguez, Phys. Rev. E **70**, 021405 (2004).

[21] P. Montgondry, J. F. Tassin, and T. Nicolai, J. Colloid Interface Sci. **283**, 397 (2005).

[22] B. Ruzicka, L. Zulian, and G. Ruocco, Phys. Rev. Lett. **93**, 258301 (2004).

[23] J.-C. Gabriel, C. Sanchez, and P. Davidson, J. Phys. Chem. **100**, 11139 (1996).

[24] D. Bonn, H. Tanaka, G. Wegdam, H. Kellay, and J. Meunier, Europhys. Lett. **45**, 52 (1998).

[25] D. Bonn, H. Kellay, H. Tanaka, G. Wegdam, and J. Meunier, Langmuir **15**, 7534 (1999).

[26] B. Abou, D. Bonn, and J. Meunier, Phys. Rev. E **64**, 021510 (2001).

[27] D. Bonn, S. Tanase, B. Abou, H. Tanaka, and J. Meunier, Phys. Rev. Lett. **89**, 015701 (2002).

[28] M. Kroon, G. H. Wegdam, and R. Sprik, Phys. Rev. E **54**, 6541 (1996).

[29] A. Knaebel, M. Bellour, J.-P. Munch, V. Viasnoff, F. Lequeux, and J. L. Harden, Europhys. Lett. **52**, 73 (2000).

[30] M. Bellour, A. Knaebel, J. L. Harden, F. Lequeux, and J.-P. Munch, Phys. Rev. E **67**, 031405 (2003).

[31] R. Bandyopadhyay, D. Liang, H. Yardimci, D. A. Sessoms, M. A. Borthwick, S. G. J. Mochrie, J. L. Harden, and R. L. Leheny, Phys. Rev. Lett. **93**, 228302 (2004).
[32] S. Kirsch, V. Frenz, W. Schärtl, E. Bartsch, and H. Sillescu, J. Chem. Phys. **104**, 1758 (1996).
[33] L. Cipelletti and D. A. Weitz, Rev. Sci. Instrum. **70**, 3214 (1999).
[34] L. Cipelletti, S. Manley, R. C. Ball, and D. A. Weitz, Phys. Rev. Lett. **84**, 2275 (2000).
[35] V. Viasnoff, F. Lequeux, and D. J. Pine, Rev. Sci. Instrum. **73**, 2336 (2002).
[36] B. J. Berne and R. Pecor, *Dynamic Light Scattering* (Wiley, New York, 1976).
[37] The principles and limitations of the method have been recently reviewed and discussed by G. D. Phillies, J. Chem. Phys. **122**, 224905 (2005).
[38] G. Maret and P. E. Wolf, Z. Phys. B: Condens. Matter **65**, 409 (1987).
[39] D. J. Pine, D. A. Weitz, P. M. Chaikin, and E. Herbolzheimer, Phys. Rev. Lett. **60**, 1134 (1988).
[40] D. A. Weitz and D. J. Pine, in *Dynamic Light Scattering: The Method and Some Applications*, edited by W. Brown, Monographs on the Physics and Chemistry of Materials, Vol. 49 (Oxford University Press, Oxford, 1993), pp. 652–720.
[41] D. Bonn, S. Tanase, B. Abou, H. Tanaka, and J. Meunier, Phys. Rev. Lett. **89**, 015701 (2002).
[42] S. Kaloun, R. Skouri, M. Skouri, J. P. Munch, and F. Schosseler, Phys. Rev. E **72**, 011403 (2005).
[43] V. Weber and F. Schosseler, Rev. Sci. Instrum. **73**, 2537 (2002).
[44] E. W. Weisstein, "Lambert W-Function." From MathWorld—A Wolfram Web Resource. http://mathworld.wolfram.com/LambertW-Function.html.
[45] T. G. Mason and D. A. Weitz, Phys. Rev. Lett. **74**, 1250 (1995).
[46] B. Schnurr, F. Gittes, F. C. MacKintosh, and C. F. Schmidt, Macromolecules **30**, 7781 (1997).
[47] G. Nisato, P. Hébraud, J.-P. Munch, and S. J. Candau, Phys. Rev. E **61**, 2879 (2000).
[48] H. Tanaka, S. Jabbari-Farouji, J. Meunier, and D. Bonn, Phys. Rev. E **71**, 021402 (2005).